Supplementary Materials

Flipped Over U: Structural Basis for dsRNA cleavage by the SARS-CoV-2 Endoribonuclease

Meredith N. Frazier[1], Isha M. Wilson[1,] Juno M. Krahn[2], Kevin John Butay[2], Lucas B. Dillard[2,3], Mario J. Borgnia[2], Robin E. Stanley[1*]

[1]Signal Transduction Laboratory, National Institute of Environmental Health Sciences, National Institutes of Health, Department of Health and Human Services, 111 T. W. Alexander Drive, Research Triangle Park, NC 27709, USA

[2]Genome Integrity and Structural Biology Laboratory, National Institute of Environmental Health Sciences, National Institutes of Health, Department of Health and Human Services, 111 T. W. Alexander Drive, Research Triangle Park, NC 27709, USA

[3]Present Address: Program in Molecular Biophysics, Johns Hopkins University, 3400 N Charles St. Baltimore, MD 21218

*Corresponding author. Email: robin.stanley@nih.gov

This File Includes:

Supplemental Figures 1-14

Supplementary Tables 1-2

Supplementary Figures and Tables

Supplementary Table 1. List of RNA oligos used in this study. All oligos were synthesized by Dharmacon (Horizon).

Oligo Name	Oligo Sequence	Purpose	Length (nt)
dsRNA_BB_f	GGAGGUAGUAGGUUGUAUAGUAGUAAGACCA GACCCUAGACCAAUUCAUGCC-Cy5	Cryo-EM, cleavage assays	52
dsRNA_BB_r	GGCAUGAAUUGGUCUAGGGUCUGGUCUUACU ACUAUACAACCUACUACCUCC-Fl	Cryo-EM, cleavage assays	52
DS10	Cy5-UUUAGAUUUCAUCUAAACGAACAAACUAAAAU GUC-Fl	Cleavage assays	35
DS11	GACAUUUUAGUUUGUUCGUUUAGAUGAAAUC UAAA	Cleavage assays	35

Supplementary Table 2. Nsp15 constructs used in this study. All mutations were synthesized by Genscript in the WT-Nsp15 backbone.

Construct	Mutation location (domain level)	First created
WT-Nsp15 (6xHis-thrombin-TEV/pet14-b)	N/A	Pillon et al(1)
Nsp15 Q19A	NTD	This study
Nsp15 Q20A	NTD	This study
Nsp15 K65A	NTD	This study
Nsp15 H235A	EndoU	Pillon et al(1)
Nsp15 H243A	EndoU	This study
Nsp15 Q245A	EndoU	This study
Nsp15 W333A	EndoU	Frazier et al(2)
Nsp15 E340A	EndoU	This study

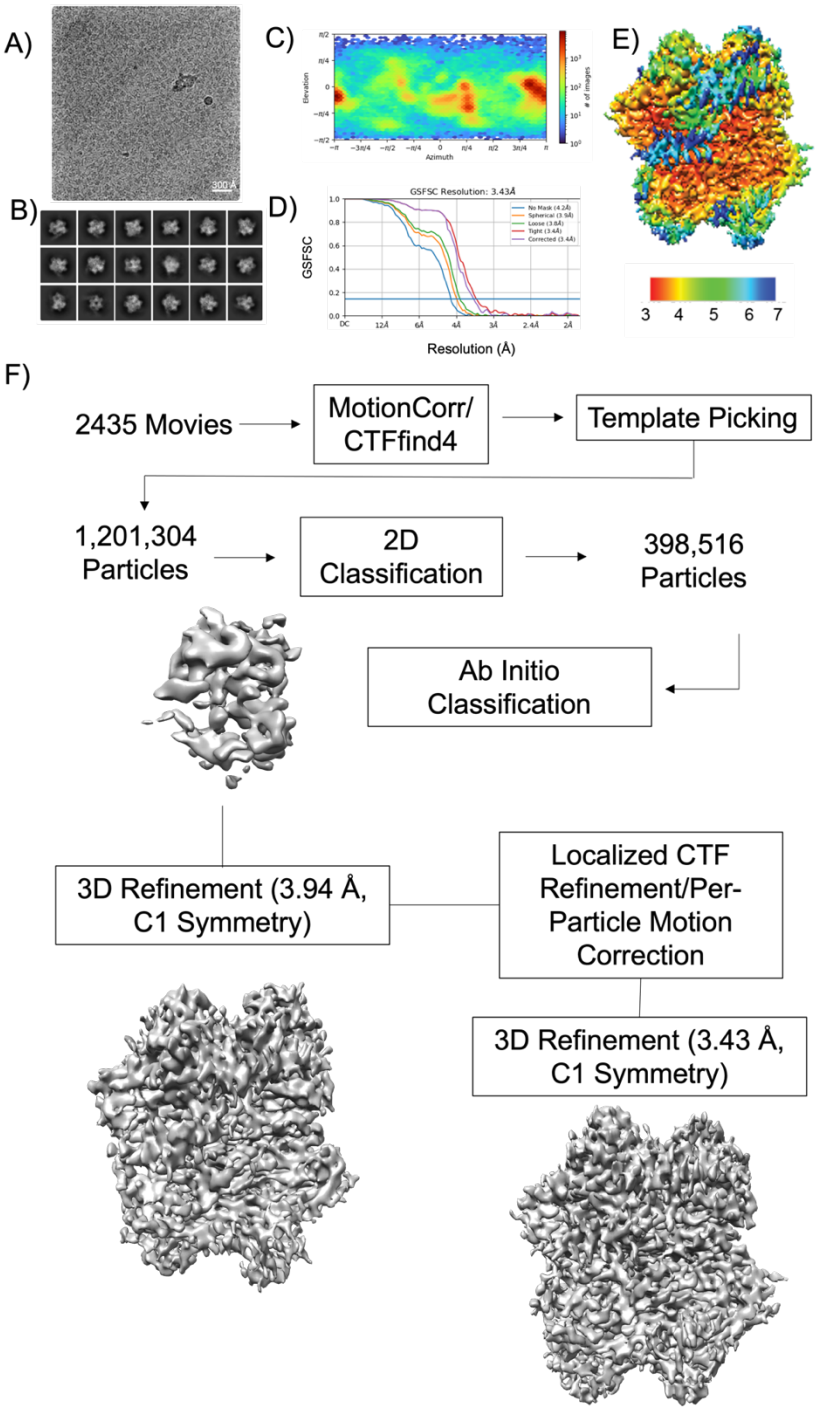

Supplementary Figure 1. Cryo-EM processing workflow. (A) A representative micrograph of Nsp15 H235A with excess 52-nt dsRNA in vitreous ice and (B) selected 2D classes generated from 738 movies collected from an UltrAuFoil R1.2/1.3 300 mesh grid. (C) Angular distribution of particles. (D) Fourier shell correlation (FSC) curve. The overall resolution is 3.43 Å according to the FSC 0.143 criteria(3). (E) Cryo-EM reconstruction colored based on local resolution calculated using cryoSparc v2 (4). (F) Cryo-EM processing workflow: picked particles (944,302) were subjected to 2D classification, 3D classification, and refinement in cryoSPARC v2 (4).

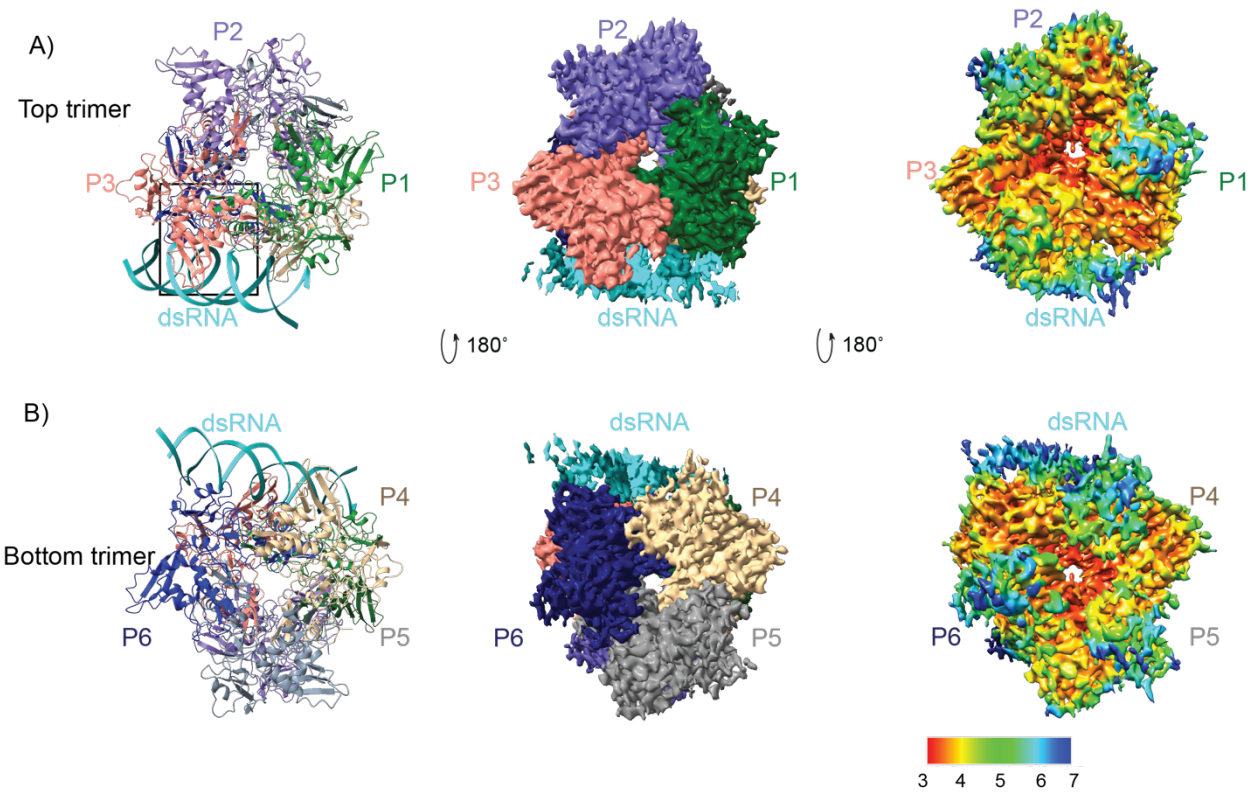

Supplementary Figure 2. Additional top and side views of the Nsp15/dsRNA complex. (**A**) Top and (**B**) bottom views of the complex in ribbon (left), EM density (middle), and local resolution (right) views.

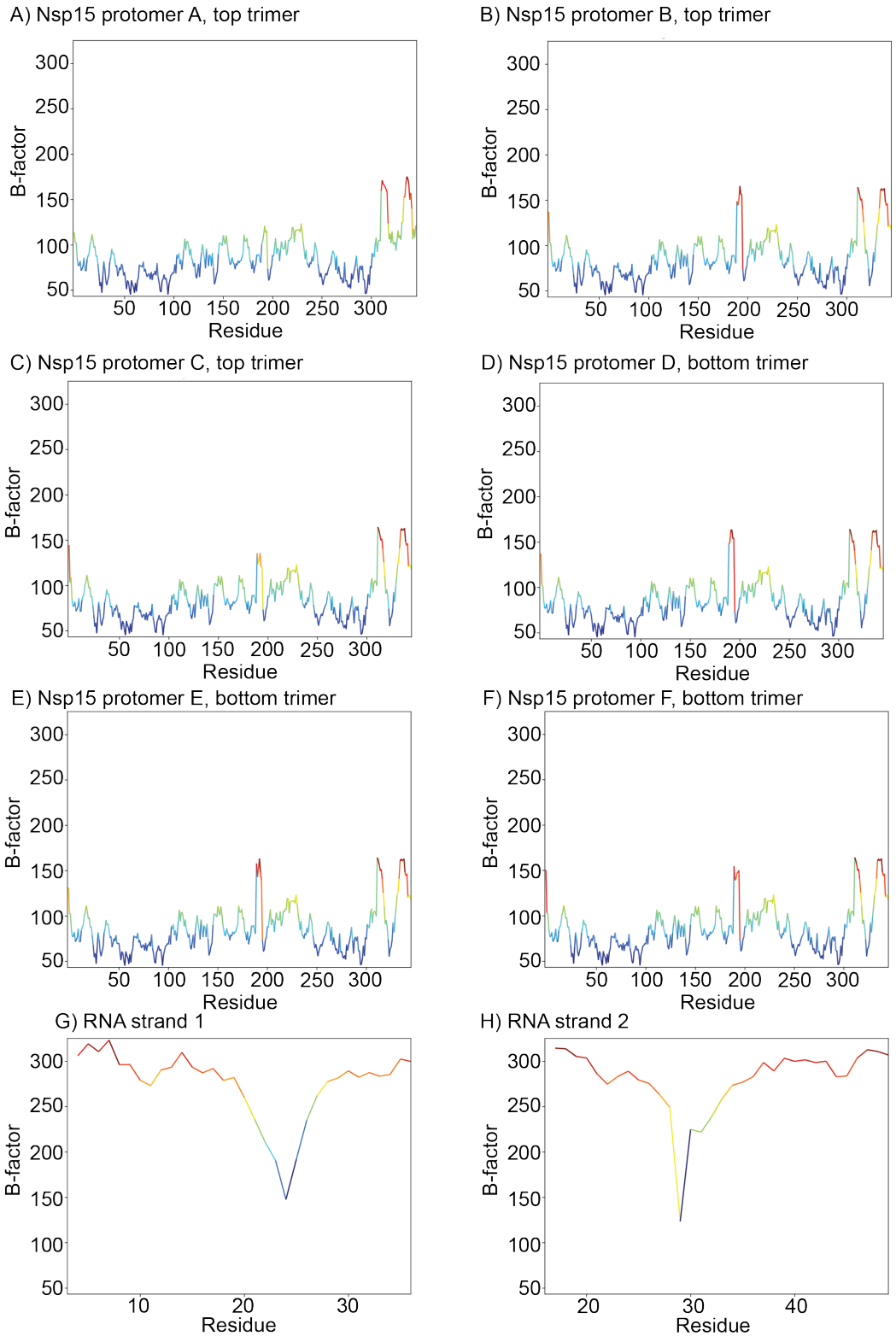

Supplementary Figure 3. Dataset 1 average B-factors plotted by residue. **A-F)** Nsp15 protomers. **G-H)** RNA strands.

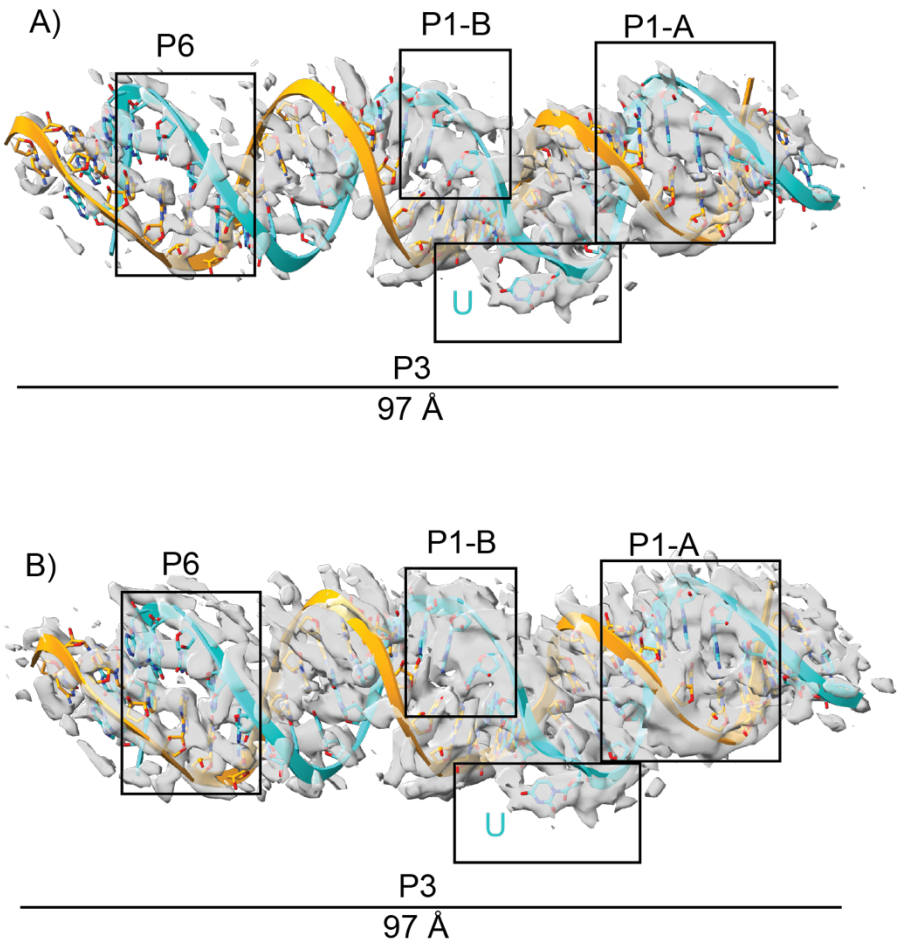

Supplementary Figure 4. Dataset 1 dsRNA density at two different contour levels: **A)** 0.45, **B)**, 0.36. Interaction sites are labeled with black boxes.

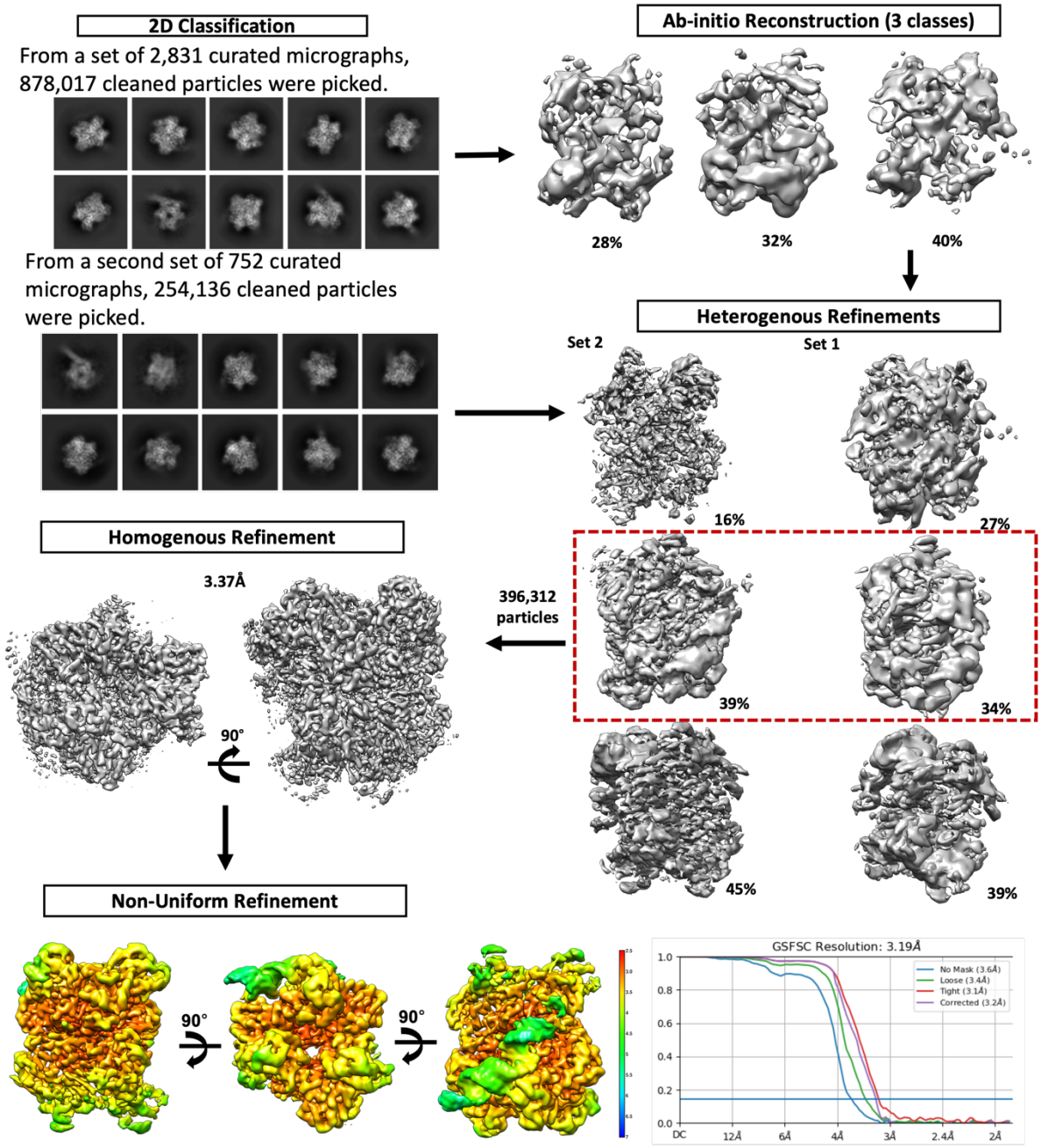

Supplementary Figure 5. Cryo-EM workflow for the combined Krios and Arctica datasets starting from curated 2D classes. The curated Arctica classes were used for *ab initio* reconstruction, which then underwent heterogeneous refinement with the Krios dataset curated particles inputted. The best class from the Krios refinement and the Arctica refinement were then combined for homogeneous refinement, followed by non-uniform refinement, resulting in a map at 3.19 Å global resolution.

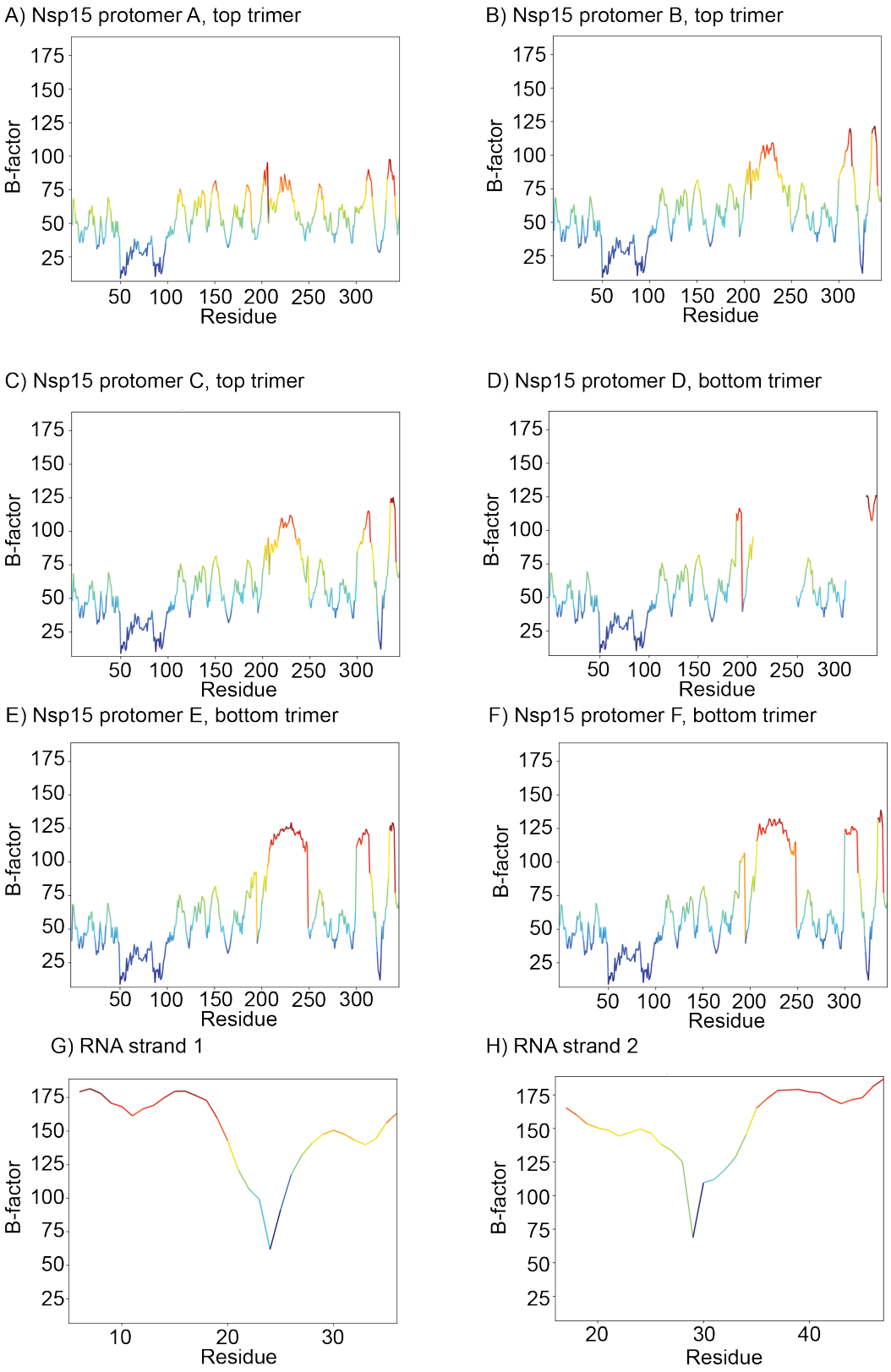

Supplementary Figure 6. Dataset 2 average B-factors plotted by residue. **A-F)** Nsp15 protomers. **G-H)** RNA strands.

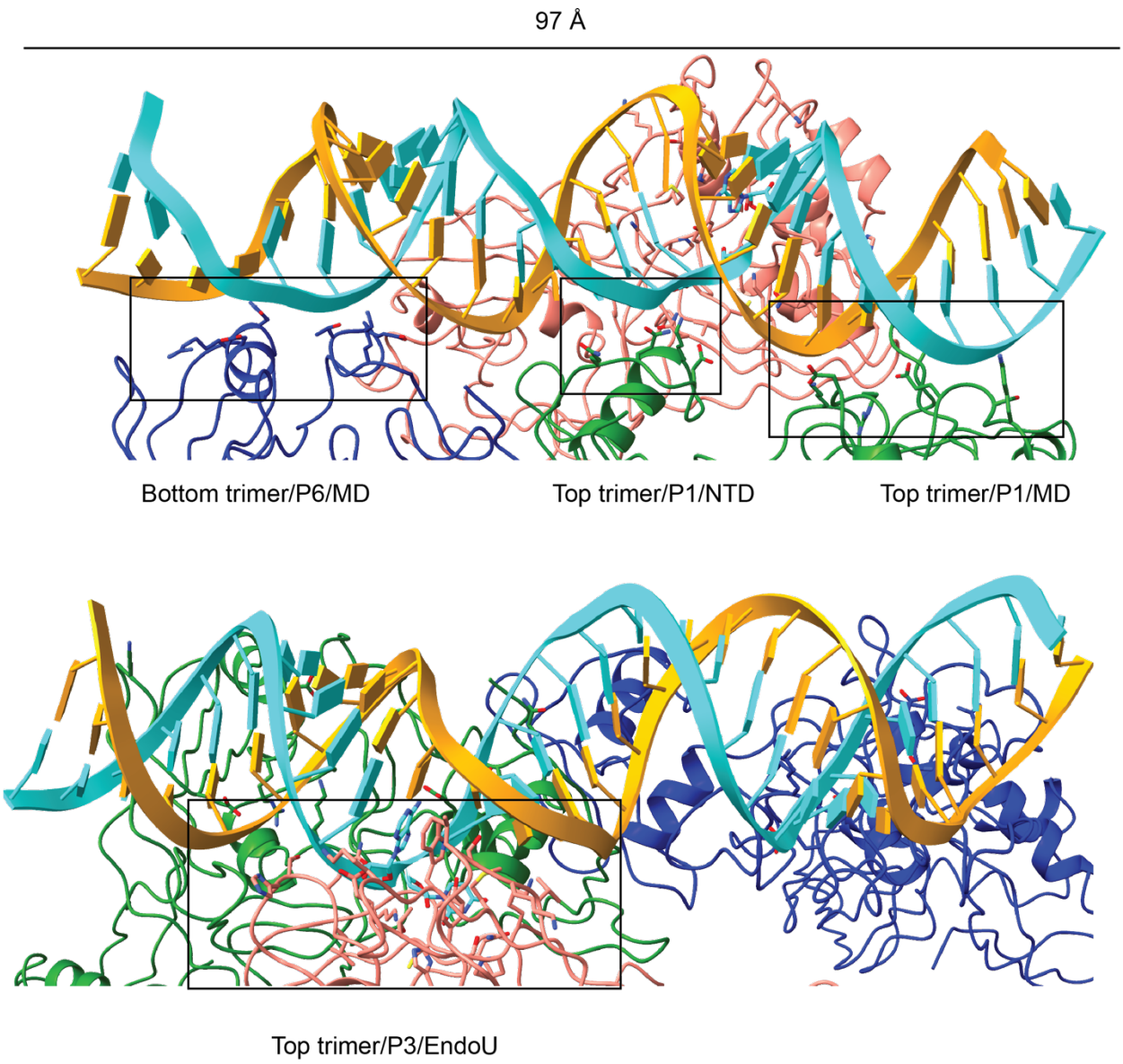

Supplementary Figure 7. Nsp15/RNA interfaces. Nsp15 interacts with dsRNA via 4 interfaces. The interfaces are denoted by black boxes, and the trimer position, protomer, and corresponding domain are listed. NTD=N-terminal domain, MD=middle domain, EndoU=catalytic C-terminal domain.

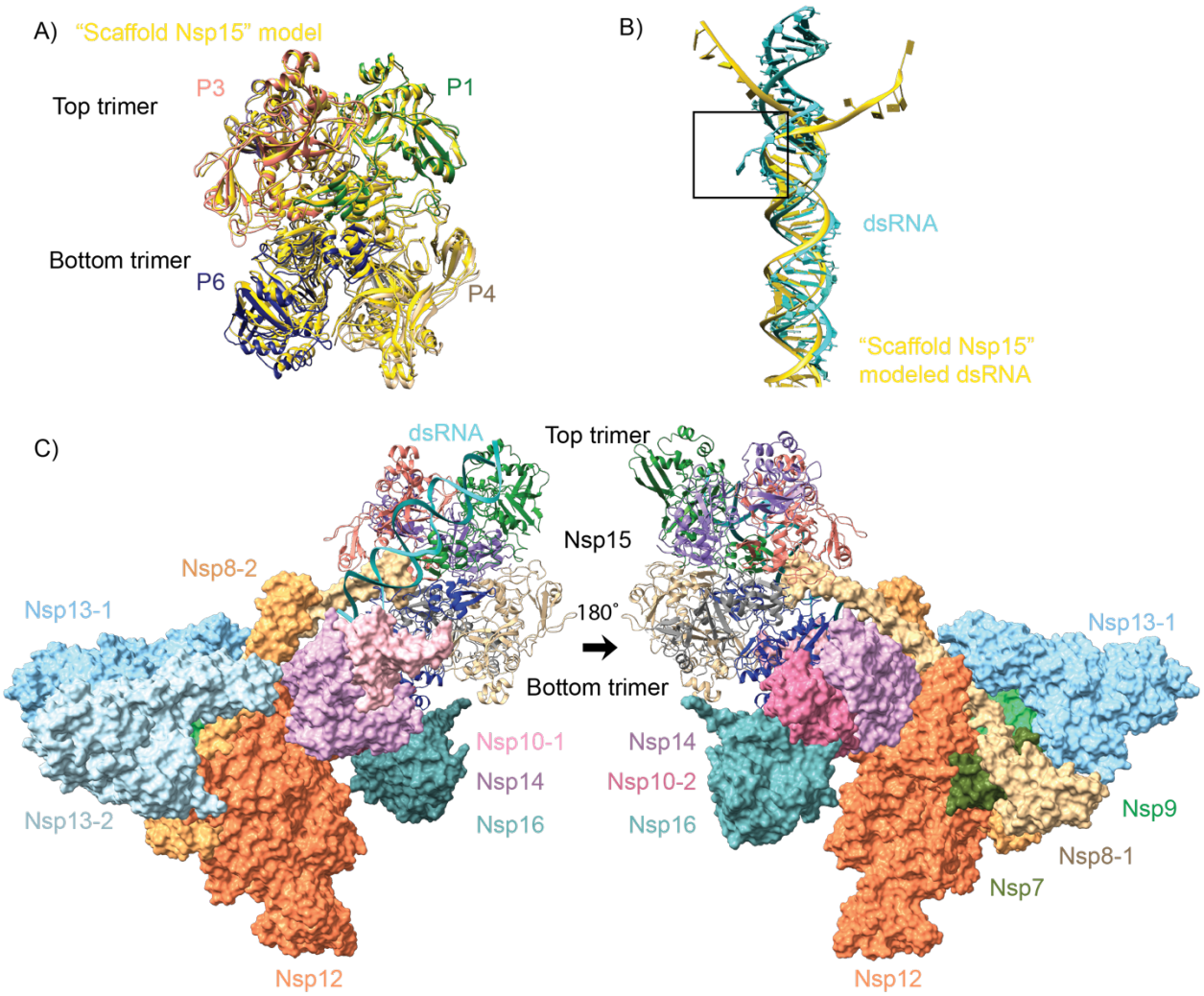

Supplementary Figure 8. Scaffold model comparison with Nsp15/dsRNA structure. A) The Nsp15 hexamer from our Arctica dataset Nsp15/dsRNA cryo-EM structure aligns well with the Nsp15 modeled as a scaffold in the RTC. (yellow). B) The dsRNA modeled into our Arctica dataset (cyan) aligns well with the dsRNA modeled into the RTC complex (yellow). Our experimental data show density for a uridine in an EndoU active site (black box). C) Extended view of the Nsp15 scaffold model (surface view(5) with our Nsp15/dsRNA structure (ribbon). For simplicity, only 1/6 of the scaffolded proteins are shown. Nsp12, the RNA-dependent RNA polymerase is shown in orange. Nsp8 (two copies, light tan and yellow-orange) and Nsp7 (olive) are polymerase accessory factors. The two copies of Nsp13, the helicase, are shown in light blue and sky blue. Nsp9, an RNA binding protein, is shown in light green. Nsp14 (light purple), a proofreading exonuclease, Nsp16 (teal), a methyltransferase, and Nsp10 (two copies, light pink and pink), their cofactor, round out the RTC scaffold model.

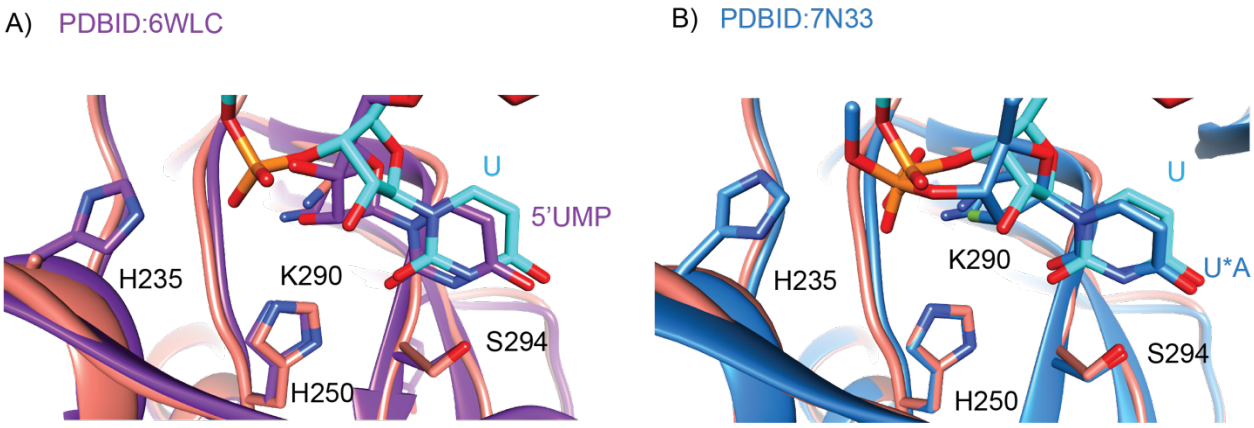

Supplementary Figure 9. Active site comparisons. A) Active site overlay of our cryo-EM structure (salmon/cyan) with an x-ray crystallography structure of Nsp15 with 5′-UMP (purple, (6)). B) Active site overlay of our cryo-EM structure (salmon/cyan) with our previously determined pre-cleavage Nsp15 cryo-EM structure (blue, (2)).

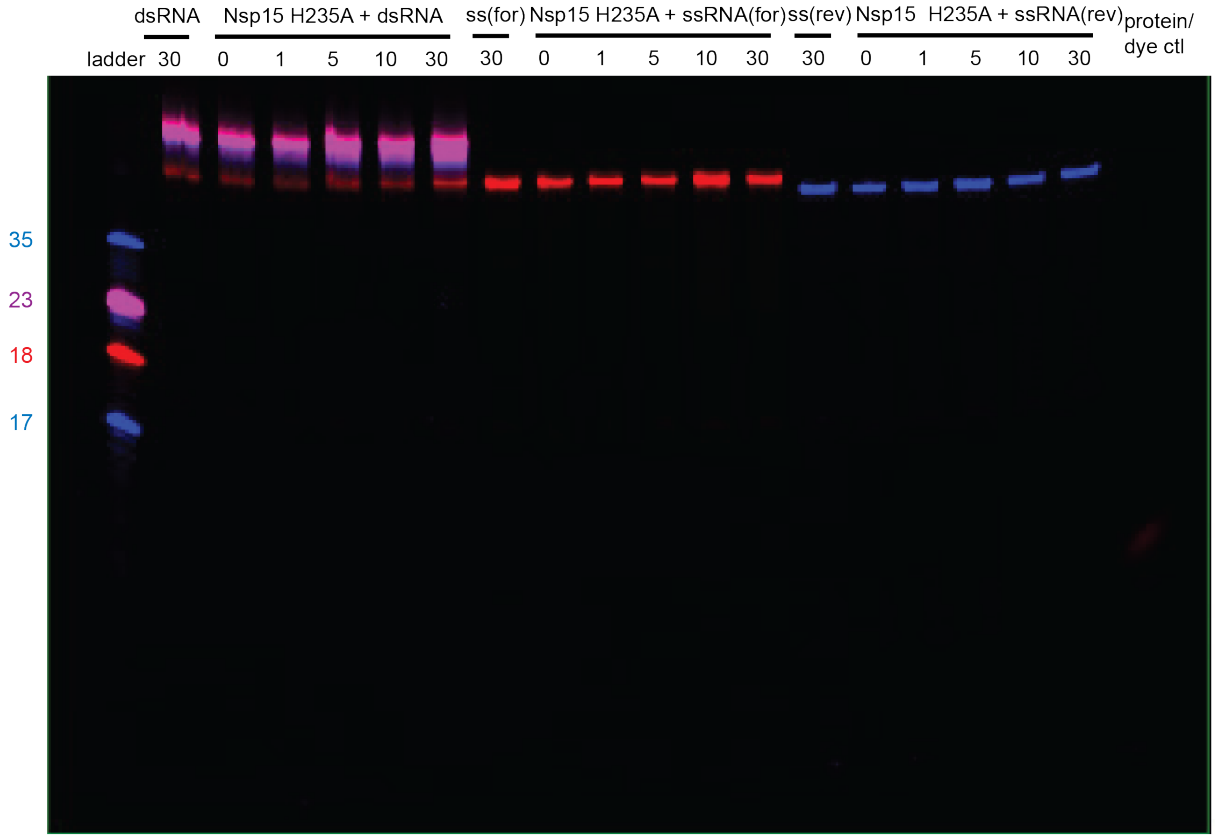

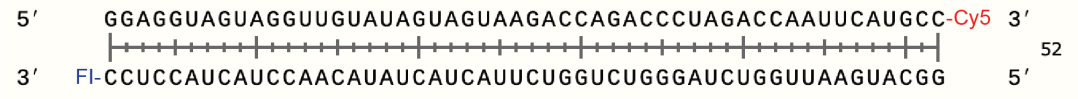

Supplementary Figure 10. Nsp15 H235A catalytic inactive cleavage control. Nsp15 H235A does not cleave the dsRNA substrate used in cryo-EM studies.

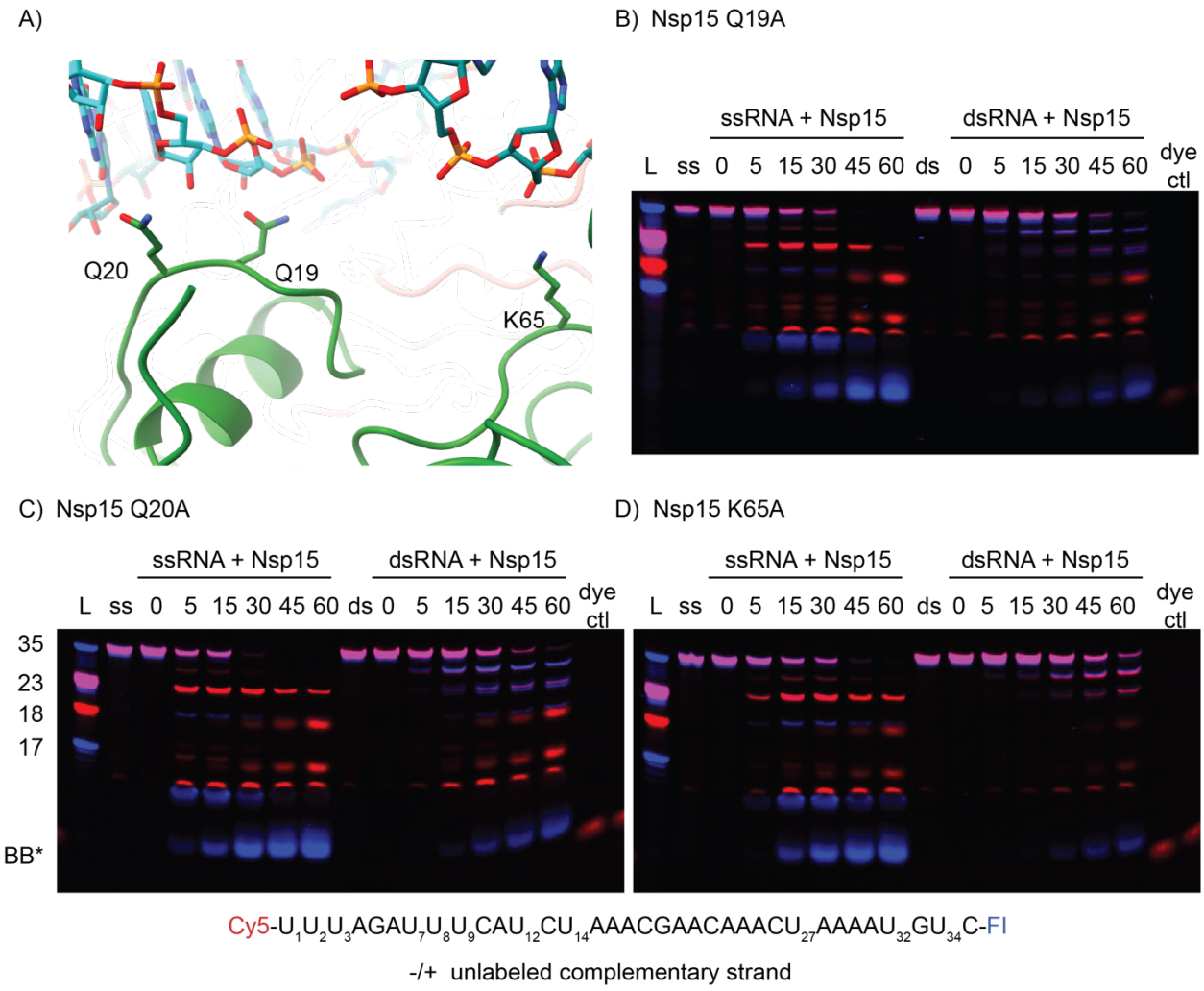

Supplementary Figure 11. Representative, complete time course cleavage reaction gels comparing ssRNA vs. dsRNA for NTD/MD Nsp15 mutants. (A) Zoomed in depiction of the NTD "platform" mutants. (**B-D**) 15% denaturing PAGE gels were used to resolve the nuclease assays. Ladder (L) nucleotide lengths are shown to the left of the gels. Bromophenol blue (BB*) runs ~8 nt in 15% denaturing gels.

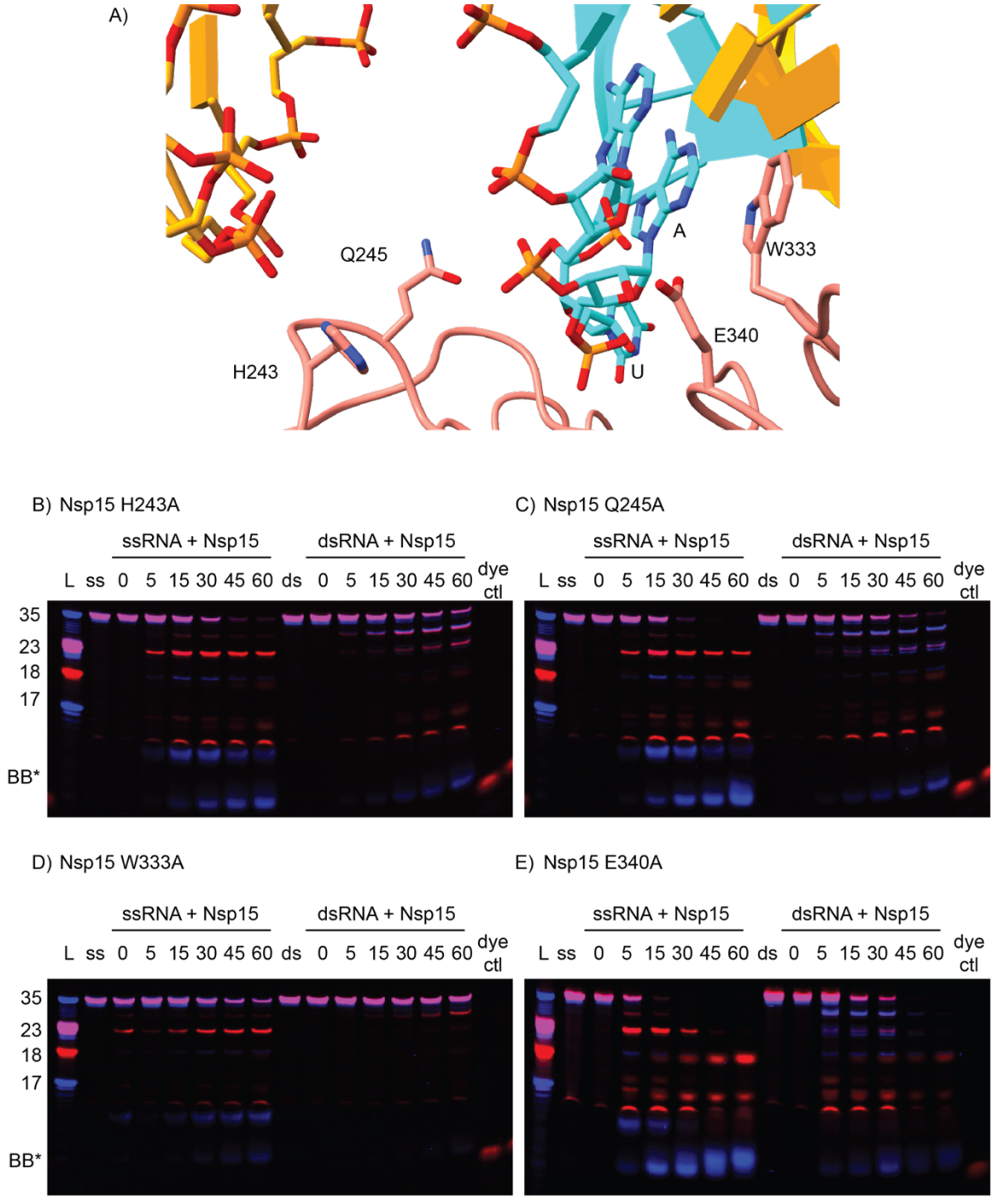

Supplementary Figure 12. Representative, complete time course cleavage reaction gels comparing ssRNA vs. dsRNA for EndoU Nsp15 mutants. (A) Zoomed in cartoon depiction of the active site, with mutated residues shown as sticks. **(B-E)** 15% denaturing PAGE gels were used to resolve the nuclease assays. Ladder (L) nucleotide lengths are shown to the left of the gels. Bromophenol blue (BB*) runs ~8 nt in 15% denaturing gels.

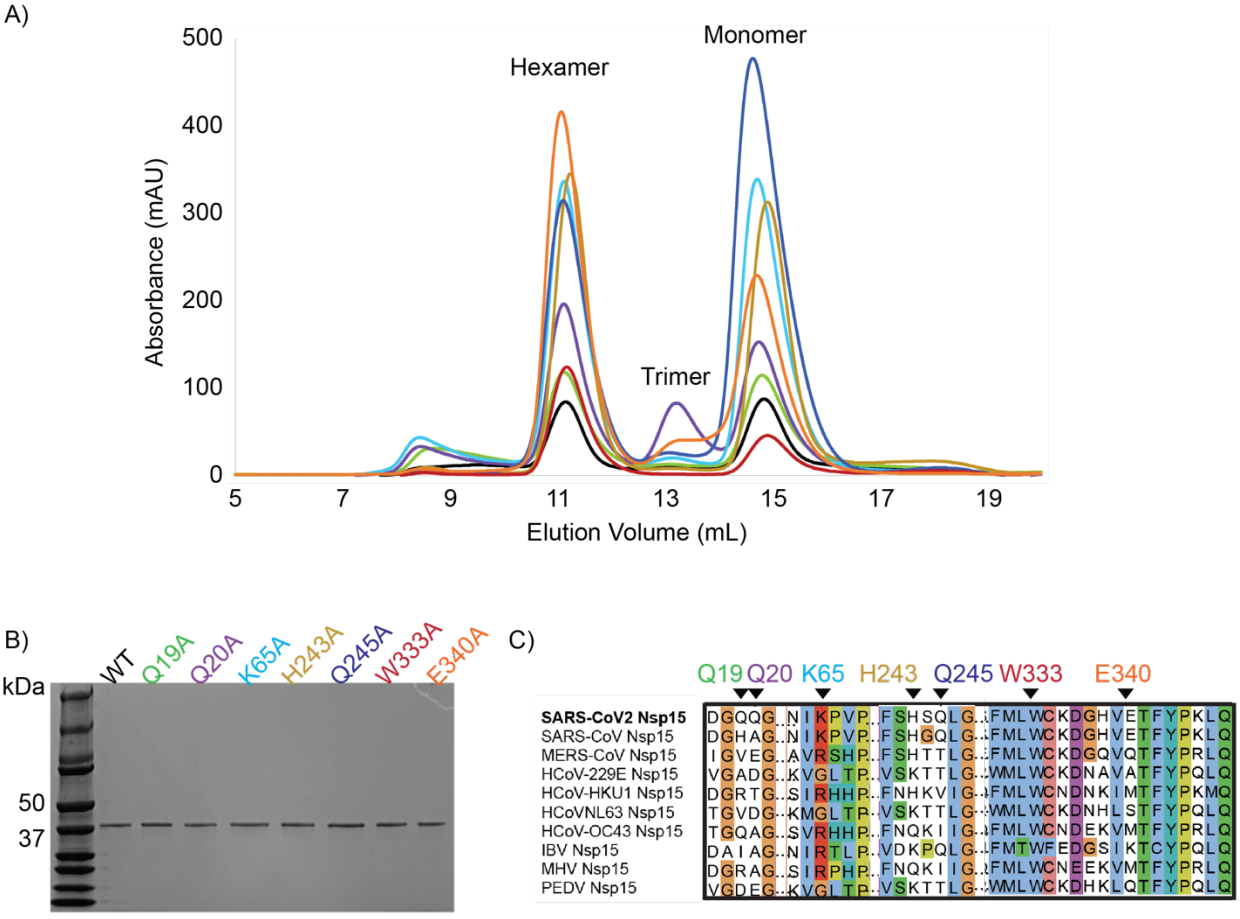

Supplementary Figure 13. Biochemical characterization of Nsp15 mutants. A) Size exclusion chromatography traces (S200 Superdex) for WT-Nsp15 and mutants. Two predominant peaks were seen for all proteins, corresponding to hexamer and monomer populations, although the proportion of each varied. Nsp15 Q20A also had a small peak corresponding to a trimer, which was inactive (data not shown). B) Summary SDS-PAGE gel for all Nsp15 constructs used in this study, showing pure protein. C) Sequence alignment for human coronaviruses and three major animal coronaviruses (infectious bronchitis virus, IBV; mouse hepatitis virus, MHV; porcine epidemic diarrhea virus, PEDV).

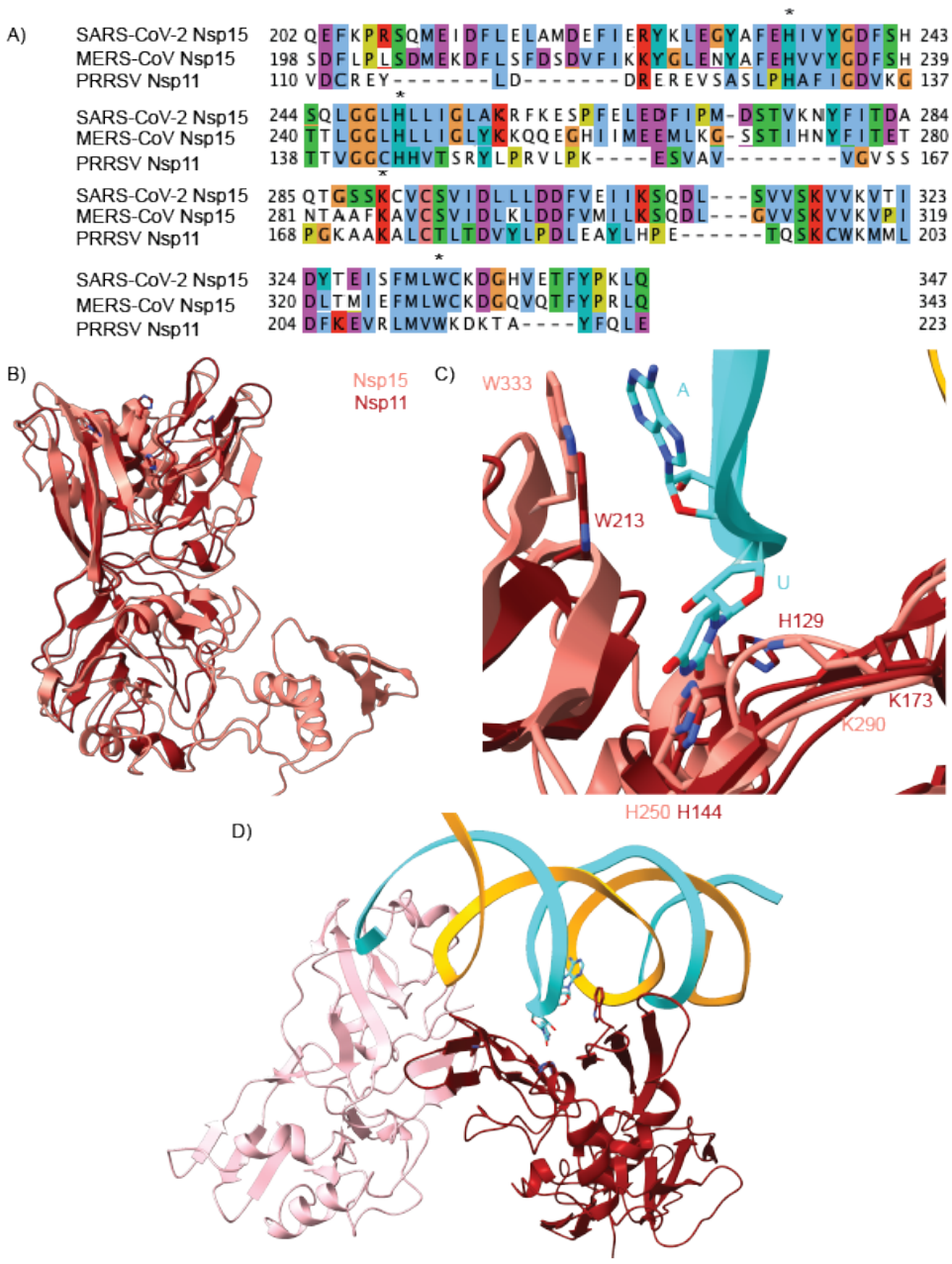

Supplementary Figure 14. Conservation of dsRNA binding. A) Sequence alignment of SARS-CoV-2 Nsp15, MERS-CoV Nsp15, and PRRSV (Porcine Reproductive and Respiratory Syndrome Virus) Nsp11. The conserved catalytic triad and π-stacking tryptophan are marked with asterisks. **B)** Superposition of protomers from SARS-CoV-2 Nsp15 (salmon, this study) and PRRSV Nsp11 (dark red, PDB: 5DA1(7)). The C-terminal EndoU domains superpose well around the active site, but otherwise the structures diverge. The overall RMSD is 7.2 Å. **C)** Zoom in of the active site overlay showing the catalytic triad and π-stacking tryptophan for Nsp11 and Nsp15 with dsRNA. **D)** The Nsp11 dimer with dsRNA modeled by superposition. The dsRNA is positioned to interact with the active site of one protomer and sits in a groove between the dimer.

Supplementary References:

1. Pillon, M.C., Frazier, M.N., Dillard, L.B., Williams, J.G., Kocaman, S., Krahn, J.M., Perera, L., Hayne, C.K., Gordon, J., Stewart, Z.D. *et al.* (2021) Cryo-EM structures of the SARS-CoV-2 endoribonuclease Nsp15 reveal insight into nuclease specificity and dynamics. *Nat Commun*, **12**, 636.
2. Frazier, M.N., Dillard, L.B., Krahn, J.M., Perera, L., Williams, J.G., Wilson, I.M., Stewart, Z.D., Pillon, M.C., Deterding, L.J., Borgnia, M.J. *et al.* (2021) Characterization of SARS2 Nsp15 nuclease activity reveals it's mad about U. *Nucleic Acids Res*, **49**, 10136-10149.
3. Rosenthal, P.B. and Henderson, R. (2003) Optimal determination of particle orientation, absolute hand, and contrast loss in single-particle electron cryomicroscopy. *J Mol Biol*, **333**, 721-745.
4. Punjani, A., Rubinstein, J.L., Fleet, D.J. and Brubaker, M.A. (2017) cryoSPARC: algorithms for rapid unsupervised cryo-EM structure determination. *Nat Methods*, **14**, 290-296.
5. Perry, J.K., Appleby, T.C., Bilello, J.P., Feng, J.Y., Schmitz, U. and Campbell, E.A. (2021) An atomistic model of the coronavirus replication-transcription complex as a hexamer assembled around nsp15. *J Biol Chem*, **297**, 101218.
6. Kim, Y., Wower, J., Maltseva, N., Chang, C., Jedrzejczak, R., Wilamowski, M., Kang, S., Nicolaescu, V., Randall, G., Michalska, K. *et al.* (2021) Tipiracil binds to uridine site and inhibits Nsp15 endoribonuclease NendoU from SARS-CoV-2. *Commun Biol*, **4**, 193.
7. Zhang, M., Li, X., Deng, Z., Chen, Z., Liu, Y., Gao, Y., Wu, W. and Chen, Z. (2017) Structural Biology of the Arterivirus nsp11 Endoribonucleases. *J Virol*, **91**.